Peer-reviewed version available at Catalysts 2018, 8, 224; doi:10.3390/catal8060224

Type of the Paper (Article, Review, Communication, etc.)

Exploring Basic Components Effect on the Catalytic Efficiency of Chevron-Phillips Catalyst in Ethylene Trimerization

Ebtehal Naji-Rad,[1] Martí Gimferrer,[2] Naeimeh Bahri-Laleh,[1,*] Mehdi Nekoomanesh-Haghighi,[1] Roghieh Jamjah[1] and Albert Poater,[2,*]

[1] Polymerization Engineering Department, Iran Polymer and Petrochemical Institute (IPPI), P.O. Box 14965/115, Tehran, Iran; n.bahri@ippi.ac.ir
[2] Institut de Química Computacional i Catàlisi, Departament de Química, Universitat de Girona, Campus de Montilivi sn, 17003 Girona, Catalonia, Spain; albert.poater@udg.edu
* Correspondence: albert.poater@udg.edu; Tel.: +34-972418358

Abstract: In the present work, effect of basic components on the energy pathway of ethylene oligomerization by landmark Chevron-Phillips catalyst has been explored in detail using density functional theory (DFT). Studied factors were chosen considering the main components of Chevron-Phillips catalyst, i.e. ligand, cocatalyst and halocarbon compounds, comprising i) the type of alkyl substituents in pyrrole ligand as methyl, iso-propyl, tert-butyl, and phenyl, as well as the simple hydrogen, and the electronwithdrawing fluoro and trifluoromethyl; ii) the number of Cl atoms in Al-compound (as $AlMe_2Cl$, $AlMeCl_2$ and $AlCl_3$) which indicates halocarbon amount and iii) cocatalyst type as alkylboron, alkylaluminium, or alkylgallium. Besides main ingredients, solvent effect, from toluene or methylcyclohexane, on oligomerization pathway was explored as well. In this regard, the full catalytic cycles for the main product (1-hexene) formation as well as side reactions, *i.e.* 1-butene release and chromacyclononane formation, were calculated on the basis of the metallacycle based mechanism. Based on results, a modification on the Chevron-Phillips catalyst system, to reach higher 1-hexene selectivity and activity, is suggested.

Keywords: Chevron-Phillips; chromium; trimerization; polymerization; reaction pathway

1. Introduction

Linear α-olefins are valuable products from petrochemical industry. They are commonly used in polyethylene industry and as plasticizer alcohols, synthetic lubricants or surfactants between other applications. Among all α-olefin monomers, 1-hexene attracted considerable attention since superior copolymer properties are achieved using it as comonomer as compared to the characteristics of 1-butene/ethylene copolymers [1]. Although 1-hexene is currently mainly produced via full-range processes, catalytic selective trimerization of ethylene to 1-hexene is an area of intense research activity [2,3,4]. Even though many companies are interested in the topic, only the Chevron–Phillips trimerization process was commercialized so far [5]. The main reasons for choosing this system over other trimerization systems, such as Cr/PNP, and Cr/SNS, are the followings: 1) high activity and selectivity for 1-hexene production, 2) its cocatalyst, *i.e.* triethylaluminium (TEAL), is much cheaper than the methylaluminoxane (MAO), 3) the synthesis of mono-dentate ligands is much easier and cheaper than tri-dentate ones, used in Chevron-Phillips catalyst and in Cr/PNP and Cr/SNS systems, respectively [6,7].

The Chevron-Phillips catalyst mainly consists of a Cr-containing precursor, a pyrrole ligand, an Al-alkyl cocatalyst and a promoter [8]. Due to the importance of the Chevron-Phillips ethylene trimerization catalyst, various experimental and theoretical studies have been conducted in the recent years, which allowed us to establish some widely accepted ideas [9,10]. For example, there is a compromise that catalytic cycle is accomplished via the

Peer-reviewed version available at Catalysts 2018, 8, 224; doi:10.3390/catal8060224

formation of metallacycle pathway in which chromium centre operates via a redox Cr(I/III) metallacyclic mechanism [11]. In fact, theoretical studies of activation energies for different stages of trimerization process revealed that the model containing Cr (I/III) redox has lower energy levels than the Cr(II/IV) species due to the more stability of the oxidation state in Cr(I/III) system [12]. This finding was further supported by the experimental results from an electron paramagnetic resonance (EPR) investigation on the same catalytic system [13].

Due to massive investigations in Chevron-Phillips catalytic system, the following precursors presented the highest activity: chromium(III) 2-ethylhexanoate ($Cr(EH)_3$) as catalyst, 2,5-dimethylpyrrole (2,5-DMP) as ligand, $AlEt_3$ as cocatalyst and a modifier [6]. Studies revealed that halocarbons containing two or more Cl atoms are good candidates in trimerization process. However, their exact role as modifiers is still in debate.

Based on the mentioned catalytic precursors, the active site model, depicted in Scheme 1, is considered as an active catalyst in the trimerization process [14,15]. This catalyst mainly consists of a pyrrole ring coordinated to the Cr centre together with a pendant R_2AlCl group σ-bonded to the pyrrole ligand, via Al-N linkage, and to the Cr metal, via Cr-Cl linkage. It is supposed that the R_2AlCl formation is produced via the simple reaction of TEAL with halocarbon promoters.

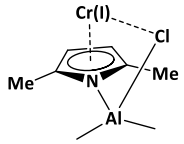

Scheme 1. Model catalyst **A**.

Despite existing proved good performance of such system, the development of improved catalysts is one of the chief areas of research in this field. For this reason, in this work a systematic study was done to shed light on: i) the effects of alkyl substituents in ligand structure, ii) the number of Cl atoms in the Al compound, iii) the revenue of Al substitution for B or Ga and iv) the solvent-type effect in the energy profile of the reaction pathway (See Scheme 2). Consequently, we have suggested modifications on the Chevron-Phillips system.

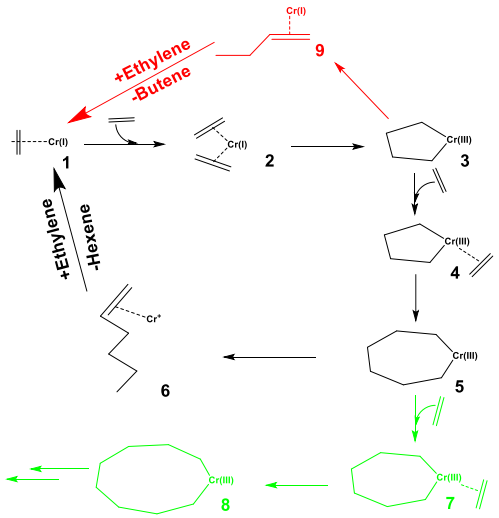

Scheme 2. Ethylene oligomerization catalytic cycle (the ligands on chromium centre are omitted for the sake of clarity).

2. Results and Discussion

The mechanism of ethylene oligomerization by the Chevron-Phillips catalyst is illustrated in Scheme 2. In this procedure, the reaction starts with the coordination of the first and second ethylene molecules into the empty site of chromium (I) (steps 1 and 2) and proceeds to the first 5-membered metallacycle formation (**3**), via oxidative addition through the transition state **TS-2-3**. In this step, the catalyst can undergo two different mechanisms: i) the main reaction, which consists of the coordination and insertion of a third ethylene molecule (**4**), leading, subsequently, to the formation of the 7-membered metallacycle (**5**). ii) the side reaction, which the elimination of 1-butene (**9**) occurs (dimerization, red diagram in Scheme 2). The main product, 1-hexene, is formed via the opening of the ring (**5**) and reductive elimination of 1-hexene from the rather unstable chroma cycloheptane (trimerization, black diagram in Scheme 2). Another side reaction also can occur in this pathway, based on first the coordination of a fourth ethylene molecule and then its insertion to the 7-membered chromic cycloheptane (**5**) leading to the 9-membered metallacycle **8** (ethylene tetramerization, green diagram in Scheme 2). Further, a two step process that leads to **3A** from **2A** was also attempted, bearing a first H transfer, but it was omitted of the analysis since kinetically was found to be much more disfavoured.

For the parent model system **A**, the energy profile we calculate in Figure 1 is very similar to that calculated earlier by Liu and coworkers [12]. The rate determining step (rds) turns out to be the transition state leading to the formation of the 7-membered metallacycle **5A** with an upper barrier placed 24.9 kcal/mol over intermediate **3A**, which is slightly more disfavoured with respect to previous results of Liu [12]. The alternative undesired reactions that lead to **8** and **9** are found to be less favoured kinetically by 8.8 and 1.6 kcal/mol, respectively. For going further into details and to unveil the complexity of the described reaction pathway, ten other model catalysts were tested in the following sections.

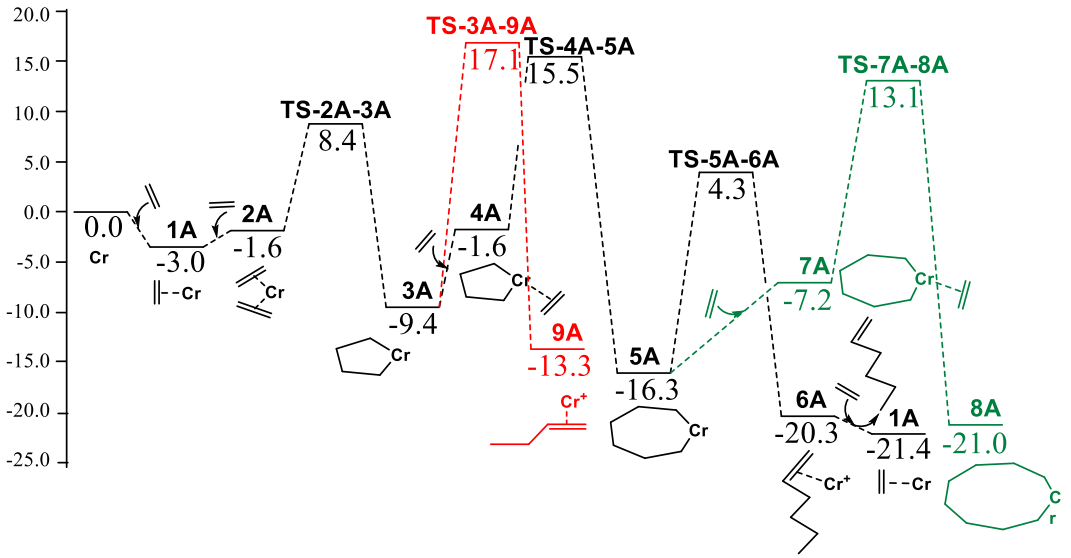

Figure 1. Calculated reaction profile for model **A** catalyst (free energies in kcal/mol). Black and red lines illustrate Gibbs free energies in solvent of ethylene tri- and dimerization, respectively, in green the alternative formation of the 9-membered ring.

2. 1. Effect of alkyl substituents on the pyrrole ligand

As a first step, the effect of the steric hindrance from dialkylpyrole type ligands on the energetic profile of the reaction pathway was elucidated. For this purpose, the three different molecular models **B**, **C** and **D** (Scheme 3), corresponding to dihydride-, diisopropyl-, and ditertbutyl-pyrrole, respectively, were employed and compared to the dimethyl-pyrrole (model **A)**. The selected models differ mainly in the alkyl group of the pyrrole ligand. First, the steric hindrance of the catalysts was analyzed by the SambVca2 Web application [16]. This application extracts the topographic maps (Figure 2), which are simple two-dimensional isocontours representing the interaction surface, by evaluating the percent buried volume (%VBur) in the single quadrants around the metal centre.

Peer-reviewed version available at Catalysts 2018, 8, 224; doi:10.3390/catal8060224

%VBur values were obtained by analyzing the steric bulk of the pyrrole ligands in the DFT optimized structures of the **A**, **B** **C** and **D** model complexes. %VBur values of 63.3, 64.6, 66.8 and 69.1 % in **B**, **A**, **C** and **D**, respectively, highlighted an obvious difference in steric bulkiness between these four complexes, with **A** clearly less bulky than **C** and much less with respect to **D**.

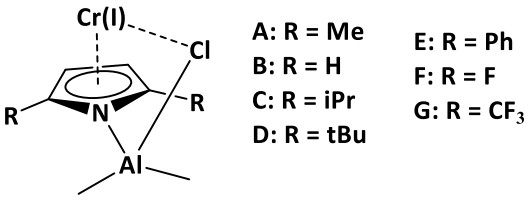

Scheme 3. Model catalysts (**A**-**G**) to study the steric and electronic effects of alkyl substituents on the pyrrole ligand.

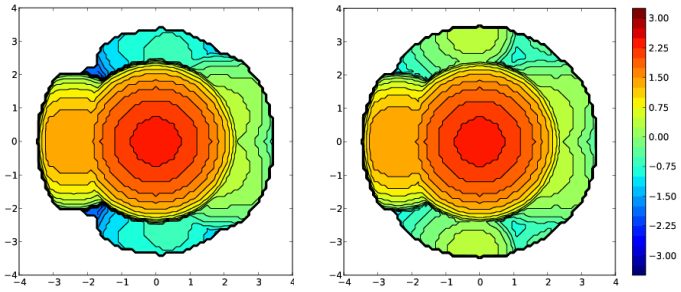

a) b)

Figure 2. Topographic steric maps of the pyrrole ligands (plane xy) for the optimized complexes a) **A** and b) **D**. The Cr atom is at the origin and the centre of mass of the pyrrole is on the z axis. The isocontour curves of the steric maps are given in Å.

The whole energy profile of the reaction pathway for ethylene oligomerization using model catalysts **B**, **C**, and **D** is shown in Table 1, together with the study of the electronic effect of the substituents on the pyrrole ligand, by means of model catalysts **E**, **F**, and **G**, bearing phenyl, fluoro and trifluoromethyl groups, respectively.

Table 1. Relative Gibbs free energies in toluene for models **A**-**G** of the ethylene dimerization, trimerization, and the formation of the 7- and also the 9-membered ring. All energies are in kcal/mol.

Model Catalyst	A	B	C	D	E	F	G
Active species	0.0	0.0	0.0	0.0	0.0	0.0	0.0
1	-3.0	-2.0	-3.2	-3.6	-0.6	2.1	2.1
2	-1.6	0.0	2.2	4.6	7.3	0.4	5.3
TS-2-3	8.4	10.4	9.6	12.1	18.3	10.4	13.9
3	-9.4	-7.7	-9.4	-7.8	-6.9	-3.8	-3.1
4	-1.6	0.2	3.6	1.2	2.8	0.8	8.3
TS-4-5	15.5	17.3	17.4	14.1	20.0	16.9	9.2
5	-16.3	-13.9	-15.5	-14.2	-13.0	-12.7	-11.8
TS-5-6	4.3	6.7	5.5	4.6	10.2	3.6	6.9
6	-20.3	-18.8	-19.8	-20.2	-17.9	-14.6	-14.8
7	-7.2	-3.2	-5.0	-0.2	-2.7	-5.9	-1.6
TS-7-8	13.1	15.0	13.4	16.8	15.3	14.0	18.0
8	-21.0	-18.9	-19.5	-18.3	-17.9	-18.2	-16.1
TS-3-9	17.1	20.8	18.4	16.1	26.0	15.7	16.7
9	-13.3	-12.5	-13.8	-13.4	-11.5	-8.1	-7.5

Peer-reviewed version available at Catalysts 2018, 8, 224; doi:10.3390/catal8060224

For a direct comparison, the energy barriers of competitive mechanisms (dimerization versus the third ethylene insertion and trimerization versus the fourth ethylene insertion) are reported in Table 2. It is worth mentioning that the formation of chromocycloheptane and chromocyclononane are the key steps to understand the 1-hexene selectivity using the mostly accepted metallacycle based mechanism proposed by Briggs for ethylene oligomerization [17,18]. The coordination of the first ethylene to the active centre was slightly exergonic by an average of 2.0-3.0 kcal/mol in all active systems, except for fluoro containing models **F** and **G**. Its explanation comes from the electron-withdrawing character of the fluorides and the trifluoromethyl groups on the pyrrole ligand, which reduces the nucleophilic capacity of the chromium centre [19].

When increasing the steric hindrance from **A** to **D**, the second monomer coordination became disfavoured. The formation of the 5-membered chromocyclopentane required to overcome energy barriers of 11.4 and 15.7 kcal/mol (**TS-2-3**) for catalysts **A** and **D**, respectively. The stable chromocyclopentane **3**, showed low tendency towards β-H transfer to Cr, *i.e.* red mechanism in Scheme 1. As a result, the formation of 1-butene from intermediate **3** required conquering an effective barrier of 26.5 kcal/mol for **A** whereas 23.9 kcal/mol for **D** model catalysts. Thus, this step is unaffected by the sterical hindrance of the sterically demanding tertbutyl groups of the latter system, which indeed even help to decrease the energy barrier. The insertion of the third ethylene that leads to the chromocycloheptane **5**, required only 24.9, 25.0, 26.8, 21.9, and 26.9 kcal/mol, for the series of **A**-**E** model catalysts, respectively, which means that the insertion of the third monomer somehow anticipated the chromocycloheptane opening. The bad performance of system **E** is attributed to the aromatic delocalization of the phenyls with the pyrrole ring. On the electronic point of view, fluoro containing electron-withdrawing groups reduce the kinetic cost to reach **5** by 4.8 and 12.6 kcal/mol comparing **B** with **F**, and **A** with **G**, respectively.

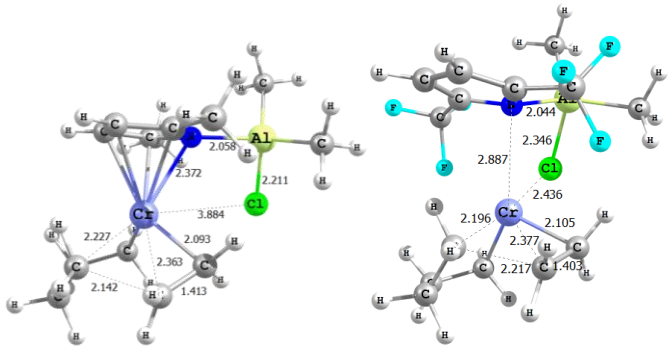

a) b)

Figure 3. 3D sketches of **TS-4-5** for complexes a) **A** and b) **G** (selected distances in Å).

In the following, the chromocycloheptane **5** required energy barriers of 20.6, 20.6, 21.0, 18.8, and 23.2 kcal/mol (**TS-5-6**) in **A**-**E** model catalysts, respectively, to release 1-hexene product. Thus, at least 5 kcal/mol lower in energy than the barrier defined by the previous **TS-4-5**. However, for the occurrence of second side reaction, *i.e.* insertion of a forth ethylene moiety into **5**, a barrier at least 5.1 kcal/mol higher in energy (**TS-7-8**) should be overcome. This fact makes the latter side reaction not affordable. The lowest preference for the formation 9-membered metallacycle **8** is hold by system **D**, for which this process is kinetically disfavoured by 12.2 kcal/mol. It was deduced from reported energy results that: by moving from dimethyl- to diisoproply- and ditertbutyl-pyrrole ligand, the selectivity toward 1-hexene formation increased. This was in line with experimental results for similar catalysts.[6,20,21] The fluorinated systems **F** and **G** increase the preference for the generation of 1-hexene, with a lower kinetic cost for **TS-5-6** of 2.1 and 2.3 kcal/mol, respectively. Even though results for model **G** are more promising than for the catalysts **A**-**F** series, actually, system **G** has some structural issues to face. Actually, the transition state **TS-4-5** was located

Preprints (www.preprints.org) | NOT PEER-REVIEWED | Posted: 26 April 2018 doi:10.20944/preprints201804.0344.v1

Peer-reviewed version available at Catalysts 2018, 8, 224; doi:10.3390/catal8060224

with the five-membered ring ligand completely dissociated from chromium (see Figure 3), which leads to the decomposition of the catalytic center afterwards, behaving potentially as a nanoparticle, partially stabilized by the chloride atom of the $Al(Me)_2Cl$ moiety. The electronwithdrawing character of the trifluoromethyl group is thus clearly competitive with the chromium affinity for the electron density of the five-membered ring.

Table 2. Effect of substituents and metal (B, Al, Ga) of the pyrrole ligand on the dimerization and trimerization energies, and 7- and 9-membered ring formation energies. All energies are in kcal/mol.

Model Catalyst	$E_{TS\text{-}4\text{-}5}$-E_3 [a]	$E_{TS\text{-}5\text{-}6}$-E_5	$E_{TS\text{-}7\text{-}8}$-E_5 [b]	$E_{TS\text{-}3\text{-}9}$-E_3
A	24.9	20.6	29.4	26.5
B	25.0	20.6	28.9	28.5
C	26.8	21.0	28.9	27.8
D	21.9	18.8	31.0	23.9
E	26.9	23.2	28.3	32.9
F	20.7	16.3	26.7	19.5
G	12.3	18.7	29.8	19.8
H	21.6	15.8	25.3	24.7
I	18.8	16.0	24.1	22.1
J	28.7	22.4	38.7	25.6
K	15.1	22.5	31.2	25.8

[a]Chromocycloheptane ring formation, [b]Chromocyclononane ring formation

2.2. Effect of the number of Cl atoms in Al compound

In the catalyst active centre, the Al compound is represented in the expected active form of $AlEt_2Cl$, although this Al based cocatalyst is usually charged to the reactor as $AlEt_3$ precursor.[6,8] It seems that the Cl-Et exchange occurs, during the catalyst activation, between $AlEt_3$ and either halocarbon promoter or catalyst precursor. Here, we assumed that at higher halocarbon/catalyst ratios, $AlMeCl_2$ and $AlCl_3$ could also be formed. As a result of such assumption, the catalytic system can be represented as Scheme 4.

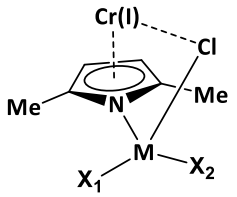

A: R = Me; $X_1 = X_2$ = Me; M = Al
H: R = Me; X_1 = Cl; X_2 = Me; M = Al
I: R = Me; $X_1 = X_2$ = Cl; M = Al
J: R = Me; $X_1 = X_2$ = Me; M = B
K: R = Me; $X_1 = X_2$ = Me; M = Ga

Scheme 4. Illustration of model catalysts (**H**-**K**).

In this section, ethylene oligomerization cycle via these catalysts was explored. Table 3 shows the Gibbs energies of the reaction pathway of ethylene oligomerization catalyzed by the model catalysts **H** and **I** with respect to **A**. Since the energy trend in the ethylene oligomerization was nearly the same as studied catalysts (**A**-**E**), here, for simplicity, we focus the analysis only on the energy barrier of the most probable products (C4, C6, and C8) formation, included in Table 2.

Table 3. Relative Gibbs free energies in toluene for the models **H-K,** with model **A** for comparison**,** for the ethylene dimerization, trimerization, and formation of the 7- and also the 9-membered ring. All energies are in kcal/mol.

Model Catalyst	A	A*	H	I	J	K
Active species	0.0	0.0	0.0	0.0	0.0	0.0
1	-3.0	-3.4	-1.9	-0.6	5.2	-3.1
2	-1.6	-2.0	-2.8	-3.2	16.6	-0.1
TS-2-3	8.4	8.0	8.2	7.2	29.1	9.9
3	-9.4	-10.0	-7.7	-6.4	-1.9	-9.4
4	-1.6	-1.9	-2.8	-4.2	11.1	0.8
TS-4-5	15.5	15.2	13.9	12.4	26.8	14.3
5	-16.3	-16.9	-13.8	-14.1	-9.4	-16.3
TS-5-6	4.3	3.9	2.0	1.9	13.0	6.2
6	-20.3	-20.9	-18.9	-18.2	-11.8	-20.4
7	-7.2	-7.6	-9.6	-10.2	11.3	-5.7
TS-7-8	13.1	12.7	11.5	10.0	29.3	14.9
8	-21.0	-21.6	-19.4	-18.8	-13.7	-21.2
TS-3-9	17.1	16.8	17.0	15.7	23.7	16.4
9	-13.3	-13.8	-12.2	-11.1	-5.8	-13.3

* Data in methylcyclohexane

As seen *vide supra*, the chromocyclopentane **3** could either undergo dimerization, with the release of the 1-butene side product, or face the third ethylene coordination to yield chromocycloheptane, **5**. Elimination of the 1-butene side product would cost 26.5, 24.7, and 22.1 kcal/mol in studied catalysts **A**, **H**, and **I**, respectively, while consecutive coordination of the third ethylene molecule, which leads to **5**, needed to overcome a much lower energy barriers of 21.6 and 18.8 kcal/mol for models **H** and **I**, respectively, to be compared with 24.9 kcal/mol for **A**. Further, Liu and coworkers stated that apart from the b-H elimination, the subsequent reduction elimination was even more expensive kinetically [12]. Thus, the energy results here clearly indicated that the third ethylene insertion represented a favourable reaction for all systems, especially for the catalysts with the higher Cl content *i.e.* **H** and **I** model systems.

Similarly, chromocycloheptanes **5** could undergo trimerization with the release of the main product 1-hexene or subsequent insertion of an ethylene moiety to yield chromocyclononane **8**. 1-hexene could be released from **5**, throughout direct reductive elimination with energy barriers of 15.8 and 16.0 kcal/mol (**TS5-6**) for models **H** and **I**, respectively, thus again the addition of chlorides on the aluminium center facilitates the reaction since for **A** this barrier is 20.6 kcal/mol. Through coordination and subsequent insertion of an ethylene molecule to **5**, complex **8** was formed with energy barriers of 29.4, 25.3, and 24.1 kcal/mol (**TS-7-8**) in models **A**, **H** and **I**, respectively. According to our theoretical results, the 1-hexene formation is more favourable for catalysts **H** and **I** with high chloride level so that the fourth ethylene coordination anticipates 1-hexene release due to its lower barrier.

Concluding this remark, according to Table 3, by increasing the number of chlorides substituted with the methyl group in the composition of the Al-compound, which indicates an increase in the halocarbon/chromium molar ratio, the trimerization requires to overcome lower energy barriers [14]. In other words, an increase in halocarbons leads to an increase on the 1-hexene selectivity [22]. It verifies higher catalyst activity towards 1-hexene formation at higher halocarbon amounts, which had already been obtained experimentally by Liu and coworkers, with the best performance using 1,1,2,2-tetrachloroethane (TCE) [23].

2.3. Effect of metal type in the cocatalyst structure

As mentioned before, the presence of an Al-compound, provided by cocatalyst, is indispensable to configure Chevron-Phillips active centre of Scheme 1. In this section, the effect of the metal type in Al-compound, along the ethylene oligomerization reaction, was

investigated. In this regard, the Al was substituted by two other elements of group III in the periodic table, boron (B) and gallium (Ga), which are considered as metalloid and metal, respectively. This produces the two new active catalysts models **J** and **K**, respectively (data included in Tables 2 and 3). To point out that the generation of **1** from the active catalyst is endergonic for system **J**, by 5.2 kcal/mol, because of the slightly higher stability of the sextet ground multiplicity state of the latter species.

Comparing quantitatively the catalyst selectivity toward the 1-butene formation with the third ethylene coordination to form **5**, the data clearly showed that progress of the reaction, *i.e.* third ethylene coordination, was more beneficial energetically for catalyst **A** (20.6 kcal/mol), than **J** and **K**, which show higher energy barriers, by 1.8 and 3.1 kcal/mol, respectively. Compare these values with the competitive fourth ethylene coordination that leads to the extension of the metallacycle size, with larger energy barriers of 16.3 and 8.7 kcal/mol for catalysts **J** and **K**, respectively. However, for boron, the catalyst would be selective towards 1-butene, rather than 1-hexene, by 3.1 kcal/mol, due to the electron deficiency. Further, since the catalytic active species the boron cocatalyst imposes structural differences with respect to the other two studied types of cocatalysts, and thus, at this point we must consider the boron behaves differently with respect to aluminium and gallium. From an energetic point of view, 1-hexene selectivity increases by the following order: Ga > Al. Concluding this section, calculations suggest a new structure, aluminium based model **I**, containing relatively electron-withdrawing groups like chlorides, as the catalyst with the highest activity (upper barrier placed at 18.8 kcal/mol), and selectivity.

2.4. Effect of solvent

Typically, ethylene oligomerization is conducted in a solvent media in both industrial and laboratory scale using Chevron-Phillips catalytic system. Typical oligomerization solvents employed in both academic laboratories and industrial settings are toluene and some saturated alkanes such as methylcyclohexane [24,25,26]. For this reason, the effect of two most widely used solvents, methylcyclohexane and toluene, on the catalytic cycle was studied.

According to the results obtained, compiled for model **A** catalyst in Table 3, the inclusion of solvent effects did not change the trend, and quantitatively the difference between both types of solvent was by far less than 1 kcal/mol in most of cases. Since many authors reported less productivity of trimerization systems in aromatic solvents such as toluene, this indicates that toluene molecules compete with the ligand for coordination to the chromium centre to form/stabilize non-selective species.

3. Conclusions

It is shown here that besides ligand and cocatalyst type, even fine details as halocarbon amount and solvent are controlling productivity and chemoselectivity. Predictive catalysis suggests a modification on the Chevron-Phillips catalyst system, to reach higher selectivity and activity, leading to 1-hexene as a product. The increase of steric hindrance on the pyrrole ring improves the catalytic performance (model **D**), as well as the addition of electron-withdrawing groups (models **F** and **G**), but when this effect is too exaggerated (model **G**), leads to decomposition by means of the decoordination of the five-membered ring ligand from chromium centres, and thus less electron-withdrawing halides like chloride improve the catalytic performance (model **I**), whereas the rather costly gallium is slightly better (model **K**) than aluminium as a metal.

4. Computational Details

To simulate the Chevron-Phillips catalytic system, a molecular model proposed by Liu et al. [12] (Scheme 1) was used. All DFT calculations were performed using the Gaussian 09 set of programs [27]. In these calculations, the B3LYP, hybrid GGA functional of Becke-Lee, Parr,

and Yang [28] was employed since as reported before, in the simulation of transition metal containing systems [29,30,31]. The electronic configuration of the studied molecules was described with the standard split valence basis set with a polarization function for H, C, Cl, Al and N (SVP keyword in Gaussian) of Ahlrichs and co-workers [32]. The quasi relativistic, small-core effective core potential of Stuttgart/Dresden, with an associated valence basis set (SDD keyword in Gaussian) was used for Cr atom [33].

Apart from Cr^{III} and Cr^{I}, unpaired electrons exist for other Cr based complexes. Due to the tendency of Cr to exhibit high spin states, the spin multiplicity was studied thoroughly and sextet was found as the ground state multiplicity for the active catalyst, whereas quadruplet for all the other studied complexes, including ethylene coordination, metallacycle and product formation, and the corresponding transition state, even though the sextet is around only 1 kcal/mol above in energy once bonded an ethylene molecule on the metal.

Solvent effects on the potential energy surfaces of oligomerization cycle were estimated based on the polarizable continuum solvation model (PCM) using methylcyclohexane and toluene as the solvents [34,35], and triple-ζ basis set (cc-pVTZ keyword in Gaussian) [36], again B3LYP, together with the Grimme D3BJ correction term to the electronic energy [37]. Thus, the free energies discussed throughout the manuscript include the electronic energies in solvent are corrected by the thermal corrections calculated in gas phase at T = 198.15 and P = 1 atm.

To determine the steric hindrance around the metal [16,38], topographical steric maps of NCH ligands were obtained by SambVca 2.0 [39,40], developed by Cavallo *et al*. The radius of the sphere around the metal centre was set to 3.5 Å, whereas for the atoms we adopted the Bondi radii scaled by 1.17, and a mesh of 0.1 Å was used to scan the sphere for buried voxels [41].

Acknowledgements

Supplementary Materials: The following are available online at www.mdpi.com/xxx/s1, xyz coordinates, energies, and 3D sketch of all computed species

Author Contributions: All authors have run calculations and contributed to write the manuscript.

Funding: This research was funded by Spanish MINECO for a project CTQ2014-59832-JIN, and EU for a FEDER fund (UNGI08-4E-003).

Acknowledgments: N. B.-L. thanks MOLNAC (www.molnac.unisa.it) for its computer facilities and Iran Polymer and Petrochemical Institute (IPPI) for the granting of the project.

351 **References**

1. Bazvand, R.; Bahri-Laleh, N.; Nekoomanesh-Haghighi, M.; Abedini, H. Highly efficient $FeCl_3$ doped $Mg(OEt)_2/TiCl_4$-based Ziegler–Natta catalysts for ethylene polymerization. *Des Monomers Polym.* **2015**, *18*, 599-610.
2. Alferov, K.A.; Babenko, I.A.; Belov, G.P. New catalytic systems on the basis of chromium compounds for selective synthesis of 1-hexene and 1-octene. *Petrol. Chem.* **2017**, *57*, 1-30.
3. Haghverdi, M.; Tadjarodi, A.; Bahri-laleh, N.; Nekoomanesh Haghighi, M. Synthesis and characterization of Ni(II) complexes bearing of 2-(1H–benzimidazol-2-yl)-phenol derivatives as highly active catalysts for ethylene oligomerization. *Appl. Organomet. Chem.* **2018**, *32*, e4015.
4. Haghverdi, M.; Tadjarodi, A.; Bahri-laleh, N.; Nekoomanesh Haghighi, M. Cobalt complexes based on 2-(1H-benzimidazol-2-yl)-phenol derivatives: preparation, spectral studies, DFT calculations and catalytic behavior toward ethylene oligomerization. *J. Coord. Chem.* **2017**, *70*, 1800-1814.
5. Agapie, T. Selective ethylene oligomerization: Recent advances in chromium catalysis and mechanistic investigations. C*hem. Rev.* **2011**, *255*, 861-880.
6. Alferov, K.A.; Belov, G.P. Meng, Y. Chromium catalysts for selective ethylene oligomerization to 1-hexene and 1-octene: Recent results. *Appl. Catal. A: Gen.* **2017**, *542*, 71-124.
7. Dixon, J.T.; Green, M.J.; Hess, F.M.; Morgan, D.H. Advances in selective ethylene trimerisation – a critical overview. *J. Organomet. Chem.* **2004**, *689*, 3641-3668.
8. Bahri-Laleh, N.; Karimi, M.; Kalantari, Z.; Fallah, M.; Hanifpour, A.; Nekoomanesh-Haghighi, M. H_2 effect in Chevron–Phillips ethylene trimerization catalytic system: an experimental and theoretical investigation. *Polym. Bull.* **2018**, https://doi.org/10.1007/s00289-017-2228-3.
9. Makhaev, V.D.; Petrova, L.A.; Alferov, K.A.; Belov, G.P. A Failed Late-Stage Epimerization Thwarts an Approach to Ineleganolide. *Russ. J. Org. Chem.* **2013**, *86*, 1819-1824.
10. T. Jiang, R. Ji, H. Chen, C. Cao, G. Mao and Y. Ning, Y. Effect of Alkylaluminum Activators on Ethylene Trimerization Based on 2,5-DMP/Cr(III)/TCE Catalyst System. *Chin. J. Chem.* **2011**, *29*, 1149-1153.
11. Gong, M.; Liu, Z.; Li, Y.; Ma, Y.; Sun, Q.; Zhang, J.; Liu, B. Selective Co-Oligomerization of Ethylene and 1-Hexene by Chromium-PNP Catalysts: A DFT Study. *Organometallics* **2016**, *35*, 972-981.
12. Yang, Y.; Liu, Z.; Cheng, R.; He, X.; Liu, B. Mechanistic DFT Study on Ethylene Trimerization of Chromium Catalysts Supported by a Versatile Pyrrole Ligand System. *Organometallics* **2014**, *33*, 2599-2607.
13. Skobelev, I.Y.; Panchenko, V.N.; Lyakin, O.Y.; Bryliakov, K.P.; Zakharov, V.A.; Talsi, E.P. In Situ EPR Monitoring of Chromium Species Formed during Cr−Pyrrolyl Ethylene Trimerization Catalyst Formation. *Organometallics* **2010**, *29*, 2943-2950.
14. Qi, Y.; Dong, Q.; Zhong, L.; Liu, Z.; Qiu, P.; Cheng, R.; He, X.; Vanderbilt, J.; Liu, B. Role of 1, 2-dimethoxyethane in the transformation from ethylene polymerization to trimerization using chromium tris (2-ethylhexanoate)-based catalyst system: a DFT study. *Organometallics* **2010**, *29*, 1588-1602.
15. Riache, N.; Dery, A.; Callens, E.; Poater, A.; Samantaray, M.; Dey, R.; Hong, J.H.; Lo, K.; Cavallo, L.; Basset, J.M. Silica-supported tungsten carbynes (=SiO)(x)W(CH)(Me)(y) (x=1, y=2; x=2, y=1): new efficient catalysts for alkyne cyclotrimerization. *Organometallics* **2015**, *34*, 690-695.
16. Poater, A.; Cosenza, B.; Correa, A.; Giudice, S.; Ragone, F.; Scarano, V.; Cavallo, L. SambVca: A Web Application for the Calculation of Buried Volumes of N-Heterocyclic Carbene Ligands. *Eur. J. Inorg. Chem.* **2009**, *2009*, 1759-1766.

17. Tobisch, S.; Ziegler, T. Catalytic Oligomerization of Ethylene to Higher Linear α-Olefins Promoted by the Cationic Group 4 [(η^5-Cp-(CMe_2-bridge)-Ph)M^{II}(ethylene)$_2$]$^+$ (M = Ti, Zr, Hf) Active Catalysts: A Density Functional Investigation of the Influence of the Metal on the Catalytic Activity and Selectivity. *J. Am. Chem. Soc.* **2004**, *126*, 9059-9071.
18. Briggs, J.R. The selective trimerization of ethylene to hex-1-ene. *J. Chem. Soc. Chem. Commun.* **1989**, 674-675.
19. Manzini, S.; Urbina-Blanco, C.A.; Nelson, D.J.; Poater, A.; Lebl, T.; Meiries, S.; Slawin, A.M.Z.; Falivene, L.; Cavallo, L.; Nolan, S.P. Evaluation of an olefin metathesis pre-catalyst with a bulky and electron-rich N-heterocyclic carbene. *J. Organomet. Chem.* **2015**, *780*, 43-48.
20. Licciulli, S.; Albahily, K.; Fomitcheva, V.; Korobkov, I.; Gambarotta, S.; Duchateau, R. A Chromium Ethylidene Complex as a Potent Catalyst for Selective Ethylene Trimerization. *Angew. Chem. Int. Ed.* **2011**, *50*, 2346-2349.
21. Araki, Y.; Nakamura, H.; Nanba, Y.; Okano, T. Process for producing α-olefin oligomer, **1999**, US Pat 5856612 A.
22. Khasbiullin, I.I.; Belov, G.P.; Kharlampidi, Kh.E.; Vil'ms, A.I. Ethylene oligomerization on the chromium ethylhexanoate-triethylaluminum-2,5-dimethylpyrrol catalytic system in the presence of carbon tetrachloride. *Petrol. Chem.* **2011**, *51*, 450–455.
23. Tang, S.; Liu, Z.; Yan, X.; Li, N.; Cheng, R.; He, X.; Liu, B. Kinetic studies on the pyrrole–Cr-based Chevron-Phillips ethylene trimerization catalyst system. *Appl. Catal. A: Gen.* **2014**, *481*, 39-48.
24. Jabri, A.; Mason, C.B.; Sim, Y.; Gambarotta, S.; Burchell, T.J.; Duchateau, R. Isolation of Single-Component Trimerization and Polymerization Chromium Catalysts: The Role of the Metal Oxidation. State. *Angew. Chem. Int. Ed.* **2008**, *47*, 9717-9721.
25. Jeon, J.Y.; Park, D.S.; Lee, D.H.; Eo, S.C.; Park, S.Y.; Jeong, M.S.; Kang, Y.Y.; Lee, J.; Lee, B.Y. A chromium precursor for the Phillips ethylene trimerization catalyst: (2-ethylhexanoate)$_2$CrOH. *Dalton Trans.* **2015**, *44*, 11004-11012.
26. Zilbershtein, T.M.; Kardash, V.A.; Suvorova, V.V.; Golovko, A.K. Decene formation in ethylene trimerization reaction catalyzed by Cr–pyrrole system. *Appl. Catal. A: Gen.* **2014**, *475*, 371-378.
27. Gaussian 09, Revision E.01, Frisch, M.J.; Trucks, G.W.; Schlegel, H.B.; Scuseria, G.E.; Robb, M.A.; Cheeseman, J.R.; Scal-mani, G.; Barone, V.; Mennucci, B.; Petersson, G.A.; Nakatsuji, H.; Caricato, M.; Li, X.; Hratchian, H.P.; Izmaylov, A.F.; Bloino, J.; Zheng, G.; Sonnenberg, J.L.; Hada, M.; Ehara, M.; Toyota, K.; Fukuda, R.; Hasegawa, J.; Ishida, M.; Nakajima, T.; Honda, Y.; Kitao, O.; Nakai, H.; Vreven, T.; Montgomery, J.A., Jr.; Peralta, J.E.; Ogliaro, F.; Bearpark, M.; Heyd, J.J.; Brothers, E.; Kudin, K.N.; Staroverov, V.N.; Kobayashi, R.; Normand, J.; Raghavachari, K.; Rendell, A.; Burant, J.C.; Iyengar, S.S.; Tomasi, J.; Cossi, M.; Rega, N.; Millam, N.J.; Klene, M.; Knox, J.E.; Cross, J.B.; Bakken, V.; Adamo, C.; Jaramillo, J.; Gomperts, R.; Stratmann, R.E.; Yazyev, O.; Austin, A.J.; Cammi, R.; Pomelli, C.; Ochterski, J.W.; Martin, R.L.; Morokuma, K.; Zakrzewski, V.G.; Voth, G.A.; Salvador, P.; Dannenberg, J.J.; Dapprich, S.; Daniels, A.D.; Farkas, Ö.; Foresman, J.B.; Ortiz, J.V.; Cioslowski, J.; Fox, D.J. Gaussian, Inc., Wallingford CT, 2009.
28. Becke, A. Density-functional exchange-energy approximation with correct asymptotic behaviour. *Phys. Rev. A* **1988**, *38*, 3098–3100.
29. Bahri-Laleh, N.; Nekoomanesh-Haghighi, M.; Mirmohammadi, S.A. A DFT study on the effect of hydrogen in ethylene and propylene polymerization using a Ti-based heterogeneous Ziegler–Natta catalyst. *J. Organomet. Chem.* **2012**, *719*, 74-79.

30. Bahri-Laleh, N.; Poater, A.; Cavallo, L.; Mirmohammadi, S.A. Exploring the Mechanism of Grignard Methathesis Polymerization of 3-alkylthiophenes. *Dalton Trans.* **2014**, *43*, 15143-15150.
31. Correa, A.; Bahri-Laleh, N.; Cavallo, L. How well can DFT reproduce key interactions in Ziegler–Natta systems? *Macromol. Chem. Phys.* **2013**, *214*, 1980-1989.
32. Schäfer, S.; Horn, H.; Ahlrichs, R. Fully Optimized Contracted Gaussian Basis Sets for Atoms Li to Kr. *J Chem Phys.* **1992**, *97*, 2571-2577.
33. Küchle, W.; Dolg, M.; Stoll, H.; Preuss, H. Energy-Adjusted Pseudopotentials for the Actinides. Parameter Sets and Test Calculations for Thorium and Thorium Monoxide. *J. Chem. Phys.* **1994**, *100*, 7535-7542.
34. Barone, V.; Cossi, M. Quantum Calculation of Molecular Energies and Energy Gradients in Solution by a Conductor Solvent Model. *J. Chem. Phys. A* **1998**, *102*, 1995-2001.
35. Tomasi, J.; Persico, M. Molecular Interactions in Solution: An Overview of Methods Based on Continuous Distributions of the Solvent. *Chem. Rev.* **1994**, *94*, 2027-2094.
36. Kendall, R.A.; Dunning Jr., T.H.; Harrison, R.J. Electron affinities of the first-row atoms revisited. Systematic basis sets and wave functions. *J. Chem. Phys.* **1992**, *96*, 6796-6806.
37. Grimme, S.; Antony, J.; Ehrlich, S.; Krieg, H. A Consistent and Accurate Ab Initio Parametrization of Density Functional Dispersion Correction (DFT-D) for the 94 Elements H-Pu. *J. Chem. Phys.* **2010**, *132*, 154104.
38. Jacobsen, H.; Correa, C.; Poater, A.; Costabile, C.; Cavallo, L. Understanding the M-(NHC) (NHC = N-Heterocyclic Carbene) Bond. *Coord. Chem. Rev.* **2009**, *253*, 687-703.
39. Falivene, L.; Credendino, R.; Poater, A.; Petta, A.; Serra, L.; Oliva, R.; Scarano, V.; Cavallo, L. SambVca 2. A Web Tool for Analyzing Catalytic Pockets with Topographic Steric Maps. *Organometallics* **2016**, *35*, 2286-2293.
40. Poater, A.; Cavallo, L. Comparing families of olefin polymerization precatalysts using the percentage of buried volume. *Dalton Trans.* **2009**, *2009*, 8878-8883.
41. Poater, A.; Ragone, F.; Giudice, S.; Costabile, C.; Dorta, R.; Nolan, S.P.; Cavallo, L. Thermodynamics of N-heterocyclic carbene dimerization: The balance of sterics and electronics. *Organometallics* **2008**, *27*, 2679-2681.